Astron. Astrophys. 315, L241–L244 (1996)

ASTRONOMY AND ASTROPHYSICS

The rich far-infrared water vapour spectrum of W Hya

M.J. Barlow[1], Nguyen-Q-Rieu[2], Truong-Bach[2], J. Cernicharo[3], E. González-Alfonso[4], X.-W. Liu[1], P. Cox[5], R.J. Sylvester[1], P.E. Clegg[6], M.J. Griffin[6], B.M. Swinyard[7], S.J. Unger[7], J.-P. Baluteau[8], E. Caux[9], M. Cohen[10], R.J. Cohen[11], R.J. Emery[7], J. Fischer[12], I. Furniss[1], W.M. Glencross[1], M.A. Greenhouse[13], C. Gry[8,20], M. Joubert[15], T. Lim[20], D. Lorenzetti[14], B. Nisini[16], A. Omont[17], R. Orfei[16], D. Péquignot[18], P. Saraceno[16], G. Serra[9], C.J. Skinner[19], H.A. Smith[13], H.J. Walker[7], C. Armand[20], M. Burgdorf[20], D. Ewart[20], A. Di Giorgio[20], S. Molinari[20], M. Price[20], S. Sidher[20], D. Texier[20], and N. Trams[20]

[1] Department of Physics and Astronomy, University College London, Gower Street, London WC1E 6BT, UK
[2] Observatoire de Paris, 61 avenue de l'Observatoire, F-75014 Paris, France
[3] IEM, Dpto Fisica Molecular, CSIC, Serrano 123, E-28006 Madrid, Spain, Also at OAN, Apartado 1143, E-28800 Alcalá de Henares, Spain
[4] Universidad de Alcalá de Henares, Dpto Física, Campus Universitario, E-28871 Alcalá de Henares, Madrid, Spain
[5] Institut d'Astrophysique Spatiale, Bât. 120, Université Paris XI, F-91405 Orsay, France
[6] Department of Physics, Queen Mary and Westfield College, Mile End Road, London E1 4NS, UK
[7] Space Science Department, Rutherford Appleton Laboratory, Chilton, Oxon OX11 0QX, UK
[8] Laboratoire d'Astronomie Spatiale, CNRS, BP 8, F-13376 Marseille Cedex 12, France
[9] Centre d'Etude Spatiale des Rayonnements, CESR/CNRS-UPS, BP 4346, F-31029 Toulouse Cedex, France
[10] Radio Astronomy Laboratory, 601 Campbell Hall, University of California, Berkeley, CA 94720, USA
[11] Nuffield Radio Astronomy Laboratories, Jodrell Bank, Macclesfield, Cheshire SK11 9DL, UK
[12] Naval Research Laboratory, Remote Sensing Division, 4555 Overlook Ave, SW, Washington, DC 20375, USA
[13] National Air and Space Museum, Smithsonian Institution, Washington, DC 20560, USA
[14] Osservatorio Astronomico di Roma, I-00040 Monte Porzio, Italy
[15] CNES, 2 place Maurice Quentin, F-75001 Paris, France
[16] CNR-Instituto di Fisica dello Spazio Interplanetario, Casella Postale 27 I-00044 Frascati, Italy
[17] Institut d'Astrophysique, 98bis boulevard Arago, F-75014 Paris, France
[18] Observatoire de Paris-Meudon, F-92190 Meudon, France
[19] Space Telescope Science Institute, 3700 San Martin Drive, Baltimore, MD 21218, USA
[20] The LWS Instrument-Dedicated Team, ISO Science Operations Centre, P.O. Box 50727, E-28080 Madrid, Spain

Received 1 August 1996 / Accepted 29 August 1996

Abstract. We present an ISO Long Wavelength Spectrometer (LWS) grating spectrum of the oxygen-rich AGB star W Hya from 43–197μm. The spectrum is dominated by a forest of water vapour emission lines, confirming that H_2O molecules are the dominant coolants of the winds of these stars. We have constructed an outflow model for the H_2O spectrum of W Hya, which successfully matches the fluxes of most of the observed H_2O lines, using an adopted wind temperature profile. These fits are sensitive to the mass loss rate, to the H_2O abundance and to the inner radius of the H_2O emitting region. The best fit parameters correspond to a mass loss rate of 6×10^{-7} $M_\odot$ yr^{-1}, inner and outer radii for the emitting region of 1.5×10^{14} and 1×10^{16} cm, and a H_2O/H_2 abundance of 8×10^{-4} for $r \leq 4.5 \times 10^{14}$ cm and 3×10^{-4} at large radii. A decrease of the H_2O/H_2 abundance in the outer envelope is consistent with the predictions of photochemical models. The availability for the first time of observations of the line fluxes from the dominant coolant species should enable improved models of the wind temperature distribution to be produced.

Key words: stars: general – stars: individual: W Hya – stars: mass loss – stars: AGB and post-AGB

1. Introduction

Water has long been believed to be an important molecule in both circumstellar and interstellar environments. It possesses a very large number of strong far-infrared (FIR) transitions, suggesting that it can act as a major, or even dominant, coolant in shocks and circumstellar outflows. Although cm-wavelength water vapour and hydroxyl maser emission from star formation regions and from cool stars has been studied for many years, the thermal conditions and the water abundance cannot be obtained

Send offprint requests to: M.J. Barlow (mjb@star.ucl.ac.uk)

[1] Based on observations with ISO, an ESA project with instruments funded by ESA Member States (especially the PI countries: France Germany, the Netherlands and the United Kingdom) and with the participation of ISAS and NASA.

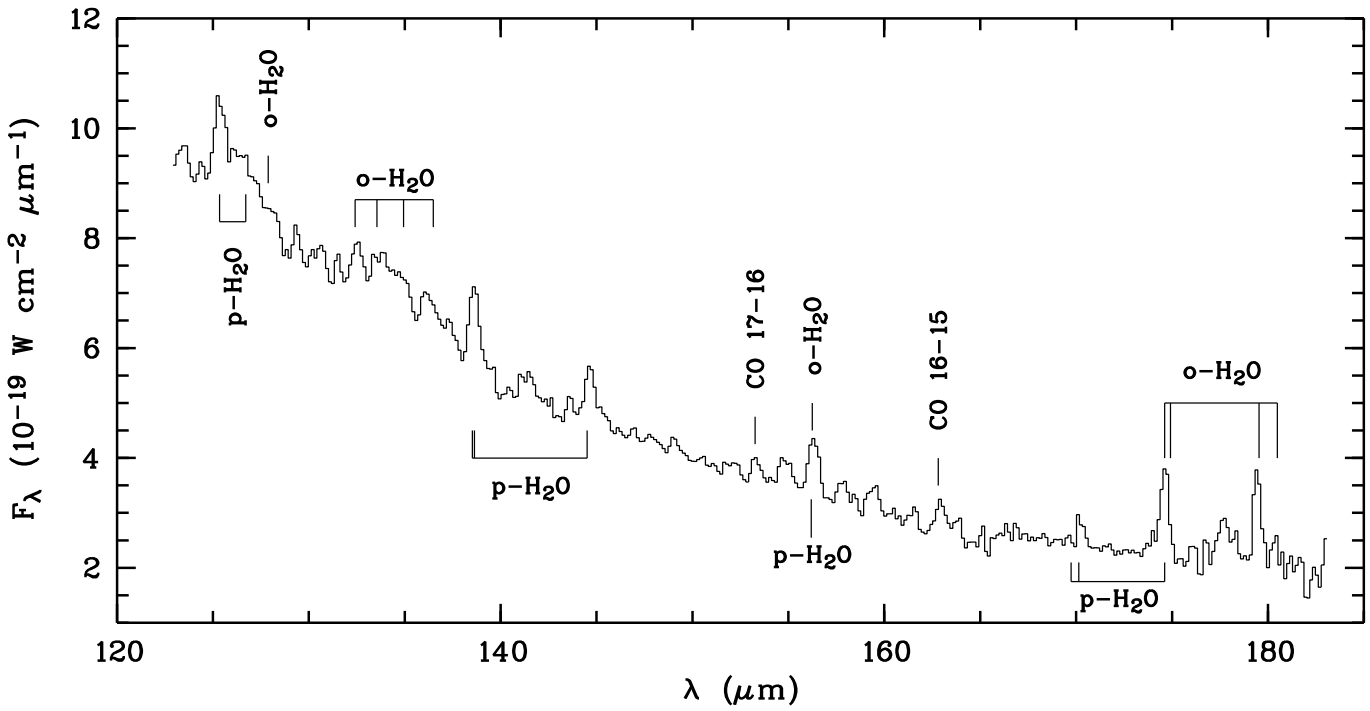

Fig. 1. The ISO LWS spectrum of W Hya between 122–183μm, with some of the strongest water vapour lines marked.

from such observations. Most of the H_2O rotational transitions occur in the FIR wavelength region, and almost all of them are predicted to be emitting thermally (e.g. Deguchi & Rieu 1990). However, the very same H_2O transitions make the Earth's atmosphere completely opaque to ground-based observations in the FIR, due to the overlap of their strong damping wings. Even at airborne altitudes, the strong Gaussian line cores of telluric water vapour lines have prevented the detection of FIR H_2O lines from astronomical sources. However, ISO's orbit puts it above such interference. The first detection of a far-IR H_2O emission line, the 179.5μm ortho-H_2O fundamental line, was made by the LWS from the planetary nebula NGC 7027 (Liu et al. 1996). Here we report the detection of many more FIR H_2O emission lines, in an LWS grating spectrum of W Hya, an oxygen-rich AGB star.

W Hya is a semi-regular variable with a spectral type of M8e-M9e. It is a strong OH and H_2O maser source (Lewis 1990, Chapman et al. 1994). Its distance, radius and effective temperature have been estimated to be 130 pc, 3.5×10^{13} cm and 2700 K, respectively (Cahn and Elitzur 1979). Its wind terminal velocity is 9 km s^{-1} (Zuckerman & Dyck 1986) and estimates for its mass loss rate vary from 10^{-7} (Loup et al 1993), 6×10^{-7} (Bujarrabal et al. 1989) to 2×10^{-6} M$_\odot$ yr^{-1} (Menten & Melnick 1991).

2. Observations

The data described here were obtained on Feb. 7 1996, during Revolution 82 of ISO (Kessler et al. 1996), using the LWS01 AOT (Clegg et al. 1996). Eight fast grating scans were obtained with 0.5 sec integration ramps at each commanded grating position. The spectra were sampled at 1/4 of a spectral resolution element, the latter being 0.3μm in second order (SW1–SW5; $\lambda\lesssim93\mu$m) and 0.6μm in first order (LW1–LW5; $\lambda\gtrsim80\mu$m). The total on-target time was 1585 sec. The absolute and relative flux calibration of the spectra was relative to Uranus (Swinyard et al. 1996). The sub-spectra from the ten LWS detectors have significant overlaps in wavelength and small scaling factors have been applied such that they joined smoothly to form a complete spectrum from 43–197μm. A portion of this spectrum is illustrated in Fig. 1.

3. Results

Inspection of Fig. 1 reveals that many rotational lines of ortho- and para-H_2O are strongly present in emission. More than 40 v = 0 ortho- and para-H_2O rotational transitions are detected, many of them blending with each other (e.g. Fig. 2). The fluxes for some of the stronger and less blended H_2O are listed in Table 1. For blended features, only the identification of the strongest component is given in the main part of the table, others are listed as footnotes. We note that there is no clear evidence for the presence of vibrationally excited rotational H_2O lines in our spectrum. No OH lines are detected, despite the fact that a significant number of OH lines have similar excitation energies to the observed H_2O lines and fall within the LWS wavelength domain. The implications of this are addressed in §4. Two CO rotational lines are detected, the 16-15 transition at 162.81μm and the 17-16 transition at 153.27μm (Table 1). The CO 15-14 transition at 173.63μm is blended with the strong o-H_2O 173.61μm line. The spectrum beyond 180μm is too noisy for the CO 14-13 186.00μm line to be detected.

4. A model for the H_2O line emission from W Hya

We have employed standard Large Velocity Gradient (LVG) models for an AGB star wind in order to try to reproduce the

Table 1. H_2O and CO FIR emission lines from W Hya

$\lambda_{vac}(\mu m)$	Identification	Det	$\lambda_{obs}(\mu m)$	$F^{a)}_{obs}$	$F^{a)}_{pred}$
57.64	p-H_2O 4_{22}–$3^{b)}_{13}$	SW2	57.64	36.2	61.6
"	"	SW3	57.66	45.2	"
58.70	o-H_2O 4_{32}–3_{21}	SW3	58.70	19.5	29.1
63.46	p-H_2O 8_{08}–$7^{c)}_{17}$	SW3	63.34	30.4	37.2
66.43	o-H_2O 3_{30}–2_{21}	SW3	66.43	22.9	28.0
67.09	p-H_2O 3_{31}–$2^{d)}_{20}$	SW3	67.19	59.8	43.4
78.74	o-H_2O 4_{23}–$3^{e)}_{12}$	SW4	78.80	28.0	34.7
"	"	SW5	78.78	28.0	"
83.28	p-H_2O 6_{06}–5_{15}	SW5	83.35	22.6	20.6
?	?	SW5	89.71	15.8	–
89.99	p-H_2O 3_{22}–2_{11}	SW5	89.87	27.3	23.5
"	"	LW1	90.02	$37.4^{f)}$	"
108.07	o-H_2O 2_{21}–1_{10}	LW1	108.07	13.0	15.0
113.69	o-H_2O 4_{14}–$3^{g)}_{03}$	LW2	113.69	17.4	15.4
125.36	p-H_2O 4_{04}–3_{13}	LW2	125.41	16.6	11.3
"	"	LW3	125.44	13.2	"
132.41	o-H_2O 4_{23}–4_{14}	LW3	132.56	5.50	4.12
144.51	p-H_2O 4_{13}–3_{22}	LW3	144.65	6.38	6.38
"	"	LW4	144.71	4.68	"
153.27	CO J=17–16	LW3	153.24	2.26	–
156.25	o-H_2O 5_{23}–$4^{h)}_{32}$	LW3	156.18	5.41	12.0
"	"	LW4	156.32	6.75	"
162.81	CO J=16–15	LW4	162.93	3.30	–
174.61	o-H_2O 3_{03}–$2^{i)}_{12}$	LW4	174.61	9.21	8.30
"	"	LW5	174.61	7.56	"
179.53	o-H_2O 2_{12}–1_{01}	LW5	179.43	8.66	10.3
180.49	o-H_2O 2_{21}–2_{12}	LW5	180.40	2.90	2.95

$^{a)}$ in 10^{-20} W cm^{-2}; $^{b)}$ also p-H_2O 8_{17}–7_{26} at 57.71μm; $^{c)}$ also o-H_2O 8_{18}–7_{07} at 63.32μm; $^{d)}$ also o-H_2O 3_{30}–3_{03} at 67.27μm; $^{e)}$ also p-H_2O 6_{15}–5_{24} at 78.93μm; $^{f)}$ flux including the unidentified line at 89.71μm; $^{g)}$ also p-H_2O 5_{33}–5_{24} at 113.95μm; $^{h)}$ also p-H_2O 3_{22}–3_{13} at 156.19μm; $^{i)}$ also o-H_2O 4_{32}–5_{05} at 174.92μm and p-H_2O 5_{33}–6_{06} at 174.61μm

observed water line fluxes under simple assumptions. Deguchi & Rieu (1990; DR90 hereafter) modelled the H_2O line emission from cool O-rich evolved stars (see also Chen & Neufeld 1995) and predicted the line fluxes for four different mass loss rates, assuming a constant fractional H_2O/H_2 abundance in the outflow of 4×10^{-4}. By chance, the parameters of the DR90 lowest mass loss rate model (3×10^{-7} M$_\odot$ yr^{-1} at a distance of 100 pc) are not too different from those inferred for W Hya. A comparison of the observed H_2O line fluxes with those predicted by this model shows agreement to within a factor of three for most lines. In this section we will discuss the results from a H_2O line model specifically tailored to W Hya.

We have used the LVG approach to compute the populations across the envelope. The ortho- and para-H_2O molecules were treated as two independent species. We considered only the lowest 45 states of o-H_2O and of p-H_2O, and used the He-H_2O collisional rates of Green et al. (1993). The collisional excitation rates of H_2O by impacts of H_2 were obtained by multiplying the H_2O + He rates by a factor of 1.35. Radiative excitation by dust emission was treated as in Elitzur et al. (1976). A dust temperature distribution $T_d \propto r^{-0.4}$, where r is the circumstellar radius,

Table 2. Model parameters for the H_2O emission from W Hya

Distance: d = 130 pc
Stellar effective temperature: T_{eff} = 2700 K
Stellar radius: R_* = 3.5 × 10^{13} cm
Mass loss rate: $\dot{M}$ = 6 × 10^{-7} M$_\odot$ y^{-1}
Wind velocity: $V_w = 9(1-0.5R_{in}/r)^{1/2}$ km s^{-1}
Envelope inner radius: R_{in} = 1.5 × 10^{14} cm
Envelope outer radius: R_{out} = 1 × 10^{16} cm
Wind kinetic temperature: T_k = 1300 K for $r \le 3R_{in}$
= $1300(3R_{in}/r)^{0.82}$ K for $r > 3R_{in}$
Water abundance: H_2O/H_2 = 8 × 10^{-4} for $r \le 6\times10^{14}$ cm
= 3 × 10^{-4} for $r > 6\times10^{14}$ cm

was assumed (Elitzur et al. 1976). This power law corresponds to a dust absorption efficiency $Q_{abs} \propto \lambda^{-1}$. The kinetic temperature distribution is taken from Goldreich & Scoville (1976).

The excitation of H_2O is dominated by collisional processes (e.g. Deguchi & Rieu 1990). The calculated spectrum is sensitive to the mass loss rate, $\dot{M}$, the H_2O/H_2 abundance ratio, and only weakly dependent on the wind velocity field and temperature structure. We first assumed a constant H_2O abundance across the envelope. The H_2O/H_2 abundance ratio and the mass loss rate $\dot{M}$ were treated as free parameters; a good fit to the observed H_2O fluxes is reached with $\dot{M} = 6\times10^{-7}M_\odot$ yr^{-1}, a total (ortho + para) water vapour abundance of $H_2O/H_2 = 4\times10^{-4}$ and an ortho-to-para ratio of 1:1. All of the observed H_2O lines are found to be very optically thick, which helps explain the ease with which the transitions from the higher rotational levels have been detected. Due to the uncertainties in both the model and the observed data, and the fact that all of the observed lines are very opaque, the H_2O ortho-to-para ratio is not well constrained and may be between 1 and 3. For low-J transitions (excitation energy $\le$ 200 cm^{-1}) the predicted lines fluxes agree within 30 per cent with the observed values. Fluxes of transitions with excitation energies $>$ 200 cm^{-1} tend to be systematically underestimated in this model. This could be due to the fact that these high-J transitions arise mainly from the inner layers of the envelope. An improved fit to these high excitation lines is achieved by adopting an enhanced H_2O/H_2 abundance ratio for this inner region, e.g. assuming H_2O/H_2 = 8 × 10^{-4} for $r \le 6\times10^{14}$ cm and H_2O/H_2 = 3 × 10^{-4} at large radii. The final model parameters are listed in Table 2. This model gives a net cooling in the wind by H_2O rotational lines of 0.17 L$_\odot$. Fig. 2 compares the observed spectra to the predicted H_2O line fluxes convolved with the instrumental line profiles. The predicted line fluxes are also compared to observed ones in Table 1. The fit is good for most of the H_2O lines, although a few of the observed lines are anomalously fainter than predicted, e.g. the 57.64μm and 58.70μm lines (Table 1) and the 156.25μm line (Table 1 & Figure 2). A decrease of the H_2O abundance in the outer part of the envelope is consistent with photochemical models, which predict that H_2O is photodissociated to OH by the interstellar UV radiation field (e.g. Huggins & Glassgold 1982). W Hya is a strong OH maser source. Since the FIR OH lines are likely to be dominated by radiation pumping by the dust continuum, the non-detection of OH lines in the LWS spectrum might be due to a low grain density and temperature in the outer envelope.

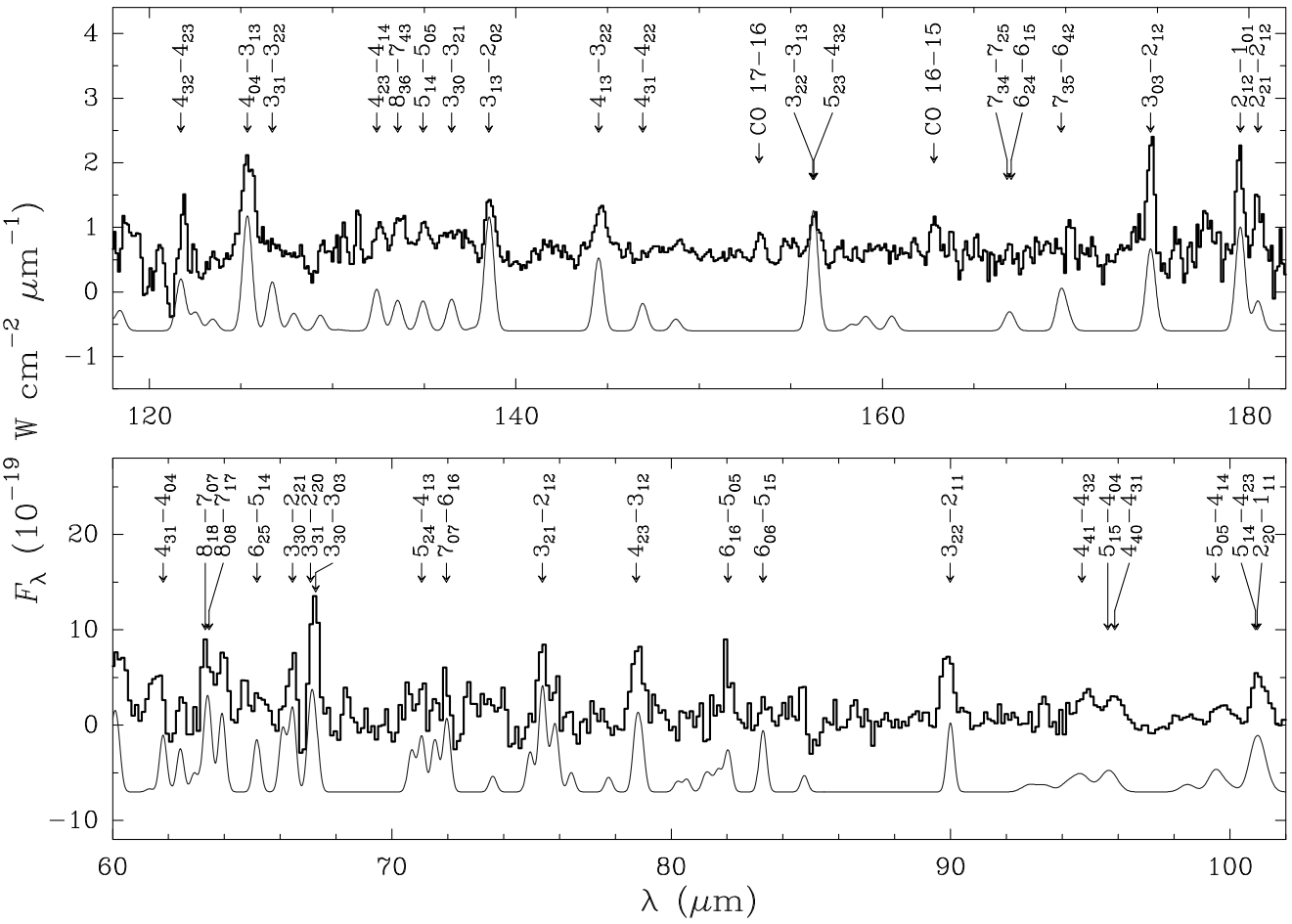

Fig. 2. The best-fit model for the H_2O line spectrum of W Hya is plotted below the continuum-subtracted observed spectrum, with the dominant transitions labelled. The parameters of the model are listed in Table 2.

The H_2O ν = 0 states can be populated via 4–9 μm radiative pumping to the ν_2 = 1 levels, which then decay to the ν = 0 states. In the current model, this process has been neglected, mainly due to the unknown vib-rotational collisional rates. However, test calculations including this excitation mechanism show that it could significantly affect the fluxes of lines from the innermost regions, i.e. those of high excitation energies. The calculations are sensitive to dust emission between 4–9μm and to the real value of the dust absorption efficiency $Q_{\rm abs}$ in this wavelength region, a poorly known quantity. The results do not depend on the FIR dust emission observed by the LWS, since the dust emission is optically thin in this wavelength domain. In fact the adopted dust temperature, $T_{\rm d} \propto r^{-0.4}$ is an upper limit and is only valid when $Q_{\rm abs}$ varies as λ^{-1} and the envelope is optically thin at all wavelengths, which is not the case at near-IR wavelengths. Clearly, a self-consistent treatment of the dust and H_2O radiative transfer is needed before the possible effect of continuum radiative pumping of H_2O vib-rotational levels can be evaluated. SWS observations of the spectrum of W Hya between 4–9μm should also be useful. Given the fact that such effects are likely to enhance the predicted H_2O line fluxes, both the mass loss rate and the H_2O/H_2 abundance ratio listed in Table 2 should be considered as upper limits. Now that the dominant cooling lines from the wind, namely those of H_2O, have been detected, it should be possible for improved models of the wind kinetic temperature distribution to be produced.

References

Bujarrabal V., Gomez-Gonzalez J., Planesas P. 1989, A&A, 219, 256
Cahn J. H., Elitzur M. 1979, ApJ, 231, 124
Chapman J. M., et al. 1994, MNRAS, 268, 475
Chen W., Neufeld D. A. 1995, ApJL, 453, L99
Clegg P. E., et al. 1996, this volume
Deguchi S, Rieu N-Q. 1990, ApJL, 360, L27
Elitzur M., et al. 1976, ApJ, 205, 384, 1976
Goldreich P., Scoville N. 1976, ApJ, 205, 144
Green S., Maluendes S., McLean A.D. 1993, ApJS, 85, 181
Huggins P., Glassgold A. E. 1982, AJ, 87, 1828
Kessler M. F., et al. 1996, this volume
Lewis B. M., 1990, AJ, 99, 710
Liu X.-W., et al. 1996, this volume
Loup C., Forveille T., Omont A., Paul J. F. 1993, A&AS, 99, 490
Menten K. M., Melnick G. J. 1991, ApJ, 377, 647
Swinyard B. M., et al. 1996, this volume
Zuckerman B., Dyck H. M. 1986, ApJ, 304, 394